

Hydronium Ion Complex of 18-Crown-6: Where Are the Protons? A Density Functional Study of Static and Dynamic Properties

Michael Bühl*[†] and Georges Wipff[‡]

Contribution from the Max-Planck-Institut für Kohlenforschung, Kaiser-Wilhelm-Platz 1, D-45470 Mülheim an der Ruhr, Germany, and UMR 7551 CNRS, Laboratoire MSM, Institut de Chimie, 4 rue Blaise Pascal, 67000 Strasbourg, France

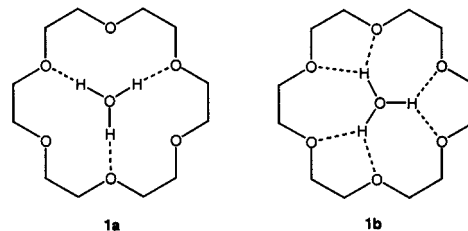
Received October 25, 2001. Revised Manuscript Received January 16, 2002

Abstract: A quantum-chemical study employing the BLYP density functional is reported for the complex of H_3O^+ with 18-crown-6. According to a Car–Parrinello molecular dynamics (CPMD) study at 340 K, the complex is quite flexible, and is characterized by three quasi-linear (two-center) hydrogen-bond interactions for most of the time. On a time scale of 10 ps, frequent inversions of H_3O^+ are observed, as well as two 120° rotations switching the hydrogen bonds from one set of crown-ether O atoms to the other. These results are consistent with density-functional studies of stationary points on the potential energy surface, which show how the crown “catalyzes” the guest’s inversion. Two close-lying minima are characterized, as well as two distinct transition states connecting them, either via H_3O^+ inversion or rotation, with barriers of 1.0 and 4.6 kcal/mol, respectively, at the BLYP/II//BLYP/6-31G* level. Orbital interactions between lone pairs on ether O atoms and hydronium σ_{OH}^* antibonding orbitals are important factors for the directionality of the hydrogen bonds.

Introduction

Cyclic polyethers are unique in their ability to bind charged atoms and small molecules selectively.¹ For instance, crown ethers can form complexes with either H_3O^+ or H_5O_2^+ , depending on the ring size.² The hydronium ion H_3O^+ has a particularly high affinity for 18-crown-6 (18c6), as evidenced by the large complexation enthalpy in the gas phase, -88.5 kcal/mol.³ This binding energy surpasses even that of alkali cations such as Na^+ or K^+ , -72 and -56 kcal/mol, respectively,⁴ and is probably matched only by that of Li^+ .⁵ For a deeper understanding of the exceptional stability of the H_3O^+ /18-crown-6 complex (**1**), numerous structural studies have been undertaken, involving the parent crown ether or derivatives thereof, together with a plethora of counterions.² In the majority of cases, the hydronium ion is found centrally located within the crown, and above the plane spanned by three of the nearest ether oxygen atoms. These data strongly suggest a pyramidal

Chart 1



geometry of H_3O^+ and symmetric coordination via three equivalent hydrogen bonds.

However, many of the X-ray crystallographic structure refinements are plagued by disorder, and the positions of the hydrogen atoms are usually refined not at all or with very low precision. It is thus not completely clear if H_3O^+ is forming three linear hydrogen bonds (**1a**, Chart 1), or if a multicenter bonded, i.e., bifurcated arrangement (**1b**) could be possible. Established examples for such bifurcated hydrogen bonds abound,⁶ and there is evidence for such bonds involving aliphatic hydrogen atoms.⁷ To our knowledge, no low-temperature neutron-diffraction study of a salt of **1** is available to address this question. Likewise, reports on accurate quantum-chemical computations are missing, even for isolated **1**. Since such data can afford information on the intrinsic bonding properties unperturbed by counterions and solvent, we decided to undertake a detailed exploration of the potential energy surface (PES) of

* Corresponding author: fax int. code + (0)208-306 2996; e-mail buehl@mpi-muelheim.mpg.de.

[†] Max-Planck-Institut für Kohlenforschung.

[‡] Laboratoire MSM, Institut de Chimie.

(1) For selected reviews see (a) Steed, J. W. *Coord. Chem. Rev.* **2001**, *215*, 171–221. (b) Bradshaw, J. S.; Izatt, R. M. *Acc. Chem. Res.* **1997**, *30*, 338–345. (c) Izatt, R. M.; Pawlak, K.; Bradshaw, J. S. *Chem. Rev.* **1991**, *91*, 1721–2085. (d) Gokel, G. *Crown Ethers and Cryptands*, Royal Society of Chemistry: Cambridge, U.K., 1991.

(2) For instance: Junk, P. C. *Rev. Inorg. Chem.* **2001**, *21*, 93–124 and references therein.

(3) Sharma, R. B.; Kebarle, P. *J. Am. Chem. Soc.* **1984**, *106*, 3913–3916.

(4) Moore, M. B.; Ray, D.; Armentrout, P. B. *J. Am. Chem. Soc.* **1999**, *121*, 417–423.

(5) According to MP2/6-31+G* computations; see Glendening, E. D.; Feller, D.; Thompson, M. A. *J. Am. Chem. Soc.* **1994**, *116*, 10657–10669.

(6) See, for instance: Jeffrey, G. A.; Saenger, W. *Hydrogen Bonding in Biological Structures*; Springer-Verlag: Berlin, 1994.

(7) Goutev, N.; Matsuura, H. *J. Phys. Chem. A* **2001**, *105*, 4741–4748.

1 with the modern tools of density-functional theory (DFT).⁸ Indeed, the calculations afford interesting insights into structural and dynamical aspects, with implications for hydrogen bonding in general.

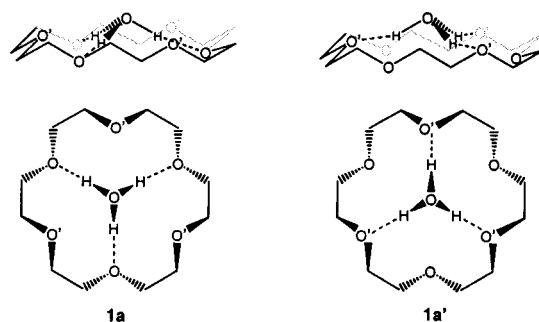
Computational Details

Geometries have been fully optimized in the given symmetry by use of the 6-31G* basis⁹ and the gradient-corrected exchange and correlation functionals according to Becke¹⁰ and Lee, Yang, and Parr¹¹ (denoted BLYP).¹² This combination of functionals has been shown to perform well for hydrogen-bonded systems.¹³ The nature of the stationary points was verified by computation of the harmonic vibrational frequencies at the BLYP/6-31G* level, which were also used unscaled for obtaining zero-point energies (ZPEs) and thermodynamic corrections to estimate enthalpies and entropies. Single-point energy evaluations were performed for the BLYP/6-31G* geometries with a somewhat larger basis set, denoted II',¹⁴ which is a (9s5p1d)/[5s4p1d] contracted Huzinaga basis on C and O, and a (5s1p)/[3s1p] and a (3s)/[2s] basis on the H atoms attached to oxygen and carbon, respectively. Energies were evaluated at the BLYP and B3LYP DFT levels, as well as on HF and MP2 levels. These computations were carried out with the Gaussian 98 program package.¹⁵ Unless otherwise noted, energies are reported at the BLYP/II' level employing the BLYP/6-31G* geometries. Complexation energies have been corrected for the basis-set superposition error (BSSE) by means of the counterpoise method.¹⁶

Additional optimizations were performed with the density-functional-based Car–Parrinello scheme¹⁷ as implemented in the CPMD program.¹⁸ The BLYP functional combination was employed, together with norm-conserving pseudopotentials generated according to the Troullier and Martins procedure¹⁹ and transformed into the Kleinman–Bylander form.²⁰ Periodic boundary conditions were imposed by use of orthorhombic supercells with box lengths of 15, 15, and 7.5 Å. Kohn–Sham orbitals were expanded in plane waves up to a kinetic energy cutoff of 80 Ry. The isolated BLYP/6-31G* geometries were taken as starting points and were reoptimized without symmetry restraints until the maximum gradient was less than 5×10^{-4} au (denoted CP-opt).

Car–Parrinello molecular dynamics simulations were performed starting from the lowest-energy structure, with a fictitious electronic mass of 600 au and a time step of 0.121 fs. Unconstrained simulations

Chart 2



(NVE ensemble) were performed over 5.5 and 11 ps at ca. 300 (\pm 30) and 340 (\pm 30) K, respectively.

Results

Minimum Energy Structures. Although a number of conformers have been characterized for 18c6,²¹ we chose the D_{3d} symmetric crown structure as a starting point, which is the form observed in all H_3O^+ complexes characterized so far. This structure has two sets of three O atoms each above and below the center of symmetry, denoted O and O', respectively, in Chart 2. For a hydronium ion approaching on the 3-fold axis, two arrangements as depicted in **1a** are conceivable, namely, with hydrogen bonds to either of these two sets. Indeed, two such minima with linear, two-center hydrogen bonds could be located, denoted **1a** and **1a'** in Chart 2 (see Table 1 for the geometrical parameters). The structure with H_3O^+ bonded to the “lower” O atoms (**1a** in Chart 2) is slightly more stable, by 0.3 kcal/mol, than the one where it is bonded to the “upper” ones (**1a'**). Both optimizations were started with imposed C_3 symmetry but converged to structures with approximate C_{3v} symmetry. The geometrical parameters of **1a** and **1a'** are similar and are indicative of strong hydrogen bonds, as evidenced, for instance, by the short O(crown)···H(H_3O^+) distances of 1.76 Å (Table 1). The hydrogen-bridged O···O separations, 2.78 and 2.76 Å for **1a** and **1a'**, respectively, are well inside the range encountered in the solid-state structures at ambient temperature, e.g., between 2.603(9) and 2.99(5) Å with $(\text{Zn/Mn})\text{Cl}_4^{2-}$ counterions,²² and are very close to the distance reported at 193 K, 2.769(2) Å.²³ The other set of nonbridged O···O separations are slightly larger, 2.91 and 2.94 Å for **1a** and **1a'**, respectively.

The hydronium ion in **1a** and **1a'** is pyramidal (H–O–H angle 113°) and its O atom is perched above the plane of the nearest set of O atoms (that is, the upper ones in both cases), for instance by 0.32 Å in **1a**, similar to what is found in many solid-state structures.^{2,24} Note that the position of the hydronium O atom with respect to the 18c6 moiety is very similar for **1a** and **1a'**, which is due to the fact that the O–H···O arrangement in **1a'** is more strongly bent than that in **1a** (166° vs 175°).

As protonated 18c6H⁺ has been characterized in the gas phase,³ we also searched for a $\text{H}_2\text{O}/18\text{c6H}^+$ complex. However, no minimum could be located that would result from an

- (8) See for instance: Koch, W.; Holthausen, M. C. *A Chemist's Guide to Density Functional Theory*; Wiley–VCH: Weinheim, Germany, 2000.
- (9) (a) Hehre, W. J.; Ditchfield, R.; Pople, J. A. *J. Chem. Phys.* **1972**, *56*, 2257–2261. (b) Hariharan, P. C.; Pople, J. A. *Theor. Chim. Acta* **1973**, *28*, 213–222.
- (10) Becke, A. D. *Phys. Rev. A* **1988**, *38*, 3098–3100.
- (11) Lee, C.; Yang, W.; Parr, R. G. *Phys. Rev. B* **1988**, *37*, 785–789.
- (12) Very similar results are obtained at the BP86/6-31G* level, i.e., employing the functionals of ref 10 and the following: (a) Perdew, J. P. *Phys. Rev. B* **1986**, *33*, 8822–8824. (b) Perdew, J. P. *Phys. Rev. B* **1986**, *34*, 7406.
- (13) Sprik, M.; Hutter, J.; Parrinello, M. *J. Chem. Phys.* **1996**, *105*, 1142–1152.
- (14) Kutzelnigg, W.; Fleischer, U.; Schindler, M. In *NMR Basic Principles and Progress*; Springer-Verlag: Berlin, 1990; Vol. 23, pp 165–262.
- (15) Frisch, M. J.; Trucks, G. W.; Schlegel, H. B.; Scuseria, G. E.; Robb, M. A.; Cheeseman, J. R.; Zakrzewski, V. G.; Montgomery, J. A., Jr.; Stratmann, R. E.; Burant, J. C.; Dapprich, S.; Millam, J. M.; Daniels, A. D.; Kudin, K. N.; Strain, M. C.; Farkas, O.; Tomasi, J.; Barone, V.; Cossi, M.; Cammi, R.; Mennucci, B.; Pomelli, C.; Adamo, C.; Clifford, S.; Ochterski, J.; Petersson, G. A.; Ayala, P. Y.; Cui, Q.; Morokuma, K.; Malick, D. K.; Rabuck, A. D.; Raghavachari, K.; Foresman, J. B.; Cioslowski, J.; Ortiz, J. V.; Stefanov, B. B.; Liu, G.; Liashenko, A.; Piskorz, P.; Komaromi, I.; Gomperts, R.; Martin, R. L.; Fox, D. J.; Keith, T.; Al-Laham, M. A.; Peng, C. Y.; Nanayakkara, A.; Gonzalez, C.; Challacombe, M.; Gill, P. M. W.; Johnson, B. G.; Chen, W.; Wong, M. W.; Andres, J. L.; Head-Gordon, M.; Replogle, E. S.; Pople, J. A. *Gaussian 98*, revision A.9; Gaussian, Inc.: Pittsburgh, PA, 1998.
- (16) Boys, S. F.; Bernardi, F. *Mol. Phys.* **1970**, *19*, 553–566.
- (17) Car, R.; Parrinello, M. *Phys. Rev. Lett.* **1985**, *55*, 2471–2474.
- (18) CPMD version 3.3a: J. Hutter, A. Alavi, T. Deutsch, M. Bernasconi, S. Goedecker, D. Marx, M. Tuckerman, and M. Parrinello, Max-Planck-Institut für Festkörperforschung and IBM Research Laboratory (1995–1999).
- (19) Troullier, N.; Martins, J. L. *Phys. Rev. B* **1991**, *43*, 1993–2006.
- (20) Kleinman, L.; Bylander, D. M. *Phys. Rev. Lett.* **1982**, *48*, 1425–1428.

- (21) (a) Dale, J. *Isr. J. Chem.* **1980**, *20*, 3–11. (b) Dobler, M. *Ionophores and their Structures*; Wiley: New York, 1981.
- (22) Chênevert, R.; Chamberland, D.; Simard, M.; Brisse, F. *Can. J. Chem.* **1990**, *68*, 797–803.
- (23) The O(hydronium) atom is disordered over two positions above and below the ring: Neumüller, B.; Plate, M.; Dehnicke, K. *Z. Kristallogr.* **1994**, *209*, 92.
- (24) Larger displacements of the hydronium oxygen, which are occasionally observed in the crystal, are probably the consequence of interactions with counterions or protic substrates present.

Table 1. Selected Geometrical Parameters and Harmonic Vibrational Frequencies of Stationary Points **1a–1d** (BLYP/6-31G* level)

parameter ^a	1a	1a'	1b	1c	1d
$r(\text{O}^*-\text{H})$	1.025	1.024	1.015	1.019	1.008
$r(\text{H}\cdots\text{O})$ short	1.762	1.756	2.008	1.727	1.992
$r(\text{H}\cdots\text{O})$ long	2.549	2.550	2.036	2.553	1.992
$r(\text{O}^*\cdots\text{O})$ short	2.784 ^b	2.759 ^b	2.834	2.744 ^b	2.819
$r(\text{O}^*\cdots\text{O})$ long	2.913	2.938	2.861	2.900	2.819
$r(\text{O}^*\cdots\text{O}_3)^c$ short	0.322	0.291	0.370	0.137	0.150
$r(\text{O}^*\cdots\text{O}_3)^c$ long	0.607	0.601	0.652	0.175	0.150
$a(\text{H}-\text{O}^*-\text{H})$	112.9	113.4	111.7	120.0	120.0
$a(\text{O}^*-\text{H}\cdots\text{O})$	174.9	165.5	136.8	174.6	136.8
NImag ^d	0	0	1	1	2
$\nu_{\text{CH}} \{+ \nu_{\text{OH}}\}$	2977 (0.06)	2993 (0.07)	2979 (0.17)	2973 (0.26)	2978 (0.13)
$\nu_{\text{CH}} \{+ \nu_{\text{OH}}\}$	2971 (0.05)	2960 (0.08)	2968 (0.09)	2953 (0.19)	2939 (0.07)
ν_{OH} asym	2873 (1.00)	2890 (1.00)	3113 (1.00)	2929 (1.00)	3206 (1.00)
$\delta_{\text{H}_2\text{O}}$ asym	1651 (0.03)	1643 (0.03)	1545 (0.14)	1594 (0.05)	1444 (0.05)
δ_{CH_2} rock	1358 (0.05)	1358 (0.05)	1356 (0.07)	1356 (0.07)	1361 (0.10)
ν_{CO} asym	1112 (0.06)	1109 (0.05)	1103 (0.00)	1110 (0.09)	1100 (0.00)
ν_{CO} asym	1057 (0.16)	1062 (0.18)	1072 (0.39)	1057 (0.26)	1069 (0.32)
$\delta_{\text{H}_2\text{O}}$ oop	1051 (0.08)	1006 (0.07)	1087 (0.10)	234i (0.02)	301i (0.04)
$\nu_{\text{CC}} + \delta_{\text{CH}_2}$ rock	965 (0.04)	963 (0.05)	958 (0.10)	962 (0.06)	1023 (0.01)
$\nu_{\text{CC}} + \delta_{\text{CH}_2}$ rock	930 (0.02)	932 (0.02)	937 (0.00)	929 (0.03)	956 (0.08)
$\delta_{\text{H}_2\text{O}}$ rock	749 (0.06)	732 (0.06)	662 (0.12)	788 (0.00)	744 (0.00)

^a Distances r are given in angstroms, angles a in degrees, and vibrational frequencies in reciprocal centimeters (relative IR intensities are shown in parentheses). O* indicates O(hydronium) atom. ^b Near-linear hydrogen bridge. ^c Distance of the O(hydronium) atom to the plane spanned by three symmetry-related O(crown) atoms; the O(hydronium) atom is perched above the two planes in **1a** and **1b**, while it is sandwiched between them in **1c** and **1d**. ^d Number of imaginary frequencies.

Table 2. Relative Energies of Stationary Points **1a'–1d**^a

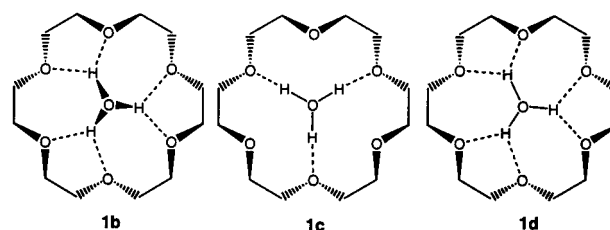
level ^b	$\text{H}_3\text{O}^+ + 18\text{c6}^c$	1a'	1b	1c	1d
BLYP/6-31G*	95.3 (92.7)	0.4	4.1	0.9	6.2
BLYP/II'	95.8 (93.2)	0.3	4.6	1.0	6.3
CP-opt ^d	92.2 (89.6)	0.2	5.1	0.8	7.0
B3LYP/II'	97.5 (94.9)	0.1	4.4	0.8	5.8
RHF/II'	90.7 (88.1)	-0.2	2.9	0.6	4.3
MP2/II'	102.0 (99.4)	0.2	4.6	1.4	7.0

^a Energies are given in kilocalories per mole, relative to **1a**. ^b BLYP/6-31G* geometries were employed, except where otherwise noted. ^c Negative binding energy; in parentheses, $-\Delta H^{298}$, as derived from the BLYP/6-31G* harmonic frequencies (experimental value 88.5 kcal/mol, ref 3). ^d Fully optimized with the CP method and the BLYP functional.

intramolecular proton transfer between hydronium and 18c6 moieties in **1a**. Attempts to optimize such a structure resulted in immediate back-transfer of the proton under recovery of **1a**, apparently without any barrier. A $\text{H}_2\text{O}/18\text{c6H}^+$ structure can be enforced by fixing the O(crown)–H distance at 1.002 Å (the value obtained for free, protonated 18c6H⁺) and optimizing all other parameters. Such a structure is, however, less stable than **1a** by 12.6 kcal/mol (13.6 kcal/mol at BLYP/6-31G*). The H_3O^+ protons in **1** are thus expected to be exclusively attached to the central hydronium oxygen atom, precluding, for instance, proton transfer to other substrates via the crown as a relay.

The computed binding energy of H_3O^+ by 18c6 is -95.8 kcal/mol (BLYP/II' energies). Inclusion of the BLYP/6-31G* zero-point and enthalpic corrections²⁵ affords an estimate for ΔH of -93.2 kcal/mol, somewhat higher than the experimental gas-phase value of -88.5 kcal/mol. This value is also overestimated when B3LYP and, in particular, MP2 energies are used. The MP2-based estimate (corrected for BSSE) is -99.4 kcal/mol (Table 2), i.e., much too high. Larger basis sets and higher levels of electron correlation are probably needed for quantitative agreement with the reported gas-phase value. Overall, the DFT methods perform quite well, in particular the BLYP functional.

(25) At the BLYP/6-31G* level, the estimated change in entropy upon complexation is $\Delta S = -40.4$ cal/(K·mol), smaller in absolute value than the experimental number, -55.8 (ref 3).

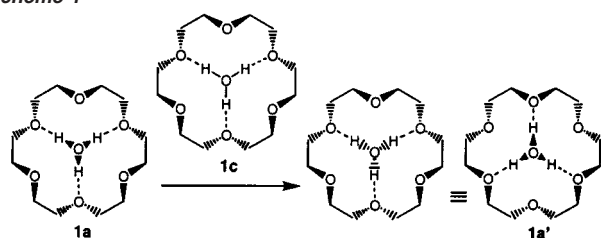
Chart 3

Incidentally, the binding enthalpy derived from the CP-opt energies, -89.6 kcal/mol, fits very well to experiment. The periodic CP computations are virtually BSSE-free due to a fixed number of plane-wave basis functions, but since there may be spurious interactions between **1** and its replicated images in the neighboring cells, the good accord with experiment may be to some extent fortuitous. Nevertheless, the energetics of complex formation are reasonably well described with the chosen methods, with the BLYP functional in particular, and the accuracy of the relative energies discussed below should be sufficient for qualitative conclusions.

Transition States for H_3O^+ Rotation and Inversion within the Complex. Structure **1b** (Chart 3) with the three-center, bifurcated hydrogen-bonding motif is not a minimum on the PES, as an optimization starting from such an arrangement collapsed to **1a**. An explicit transition-state search confirmed that **1b** is the saddle point for rotation of H_3O^+ from one 3-fold set of O(crown) atoms to the other; that is, from **1a** to **1a'**. The computed barrier on the PES is small but noticeable, 4.6 kcal/mol (note the consistency of the post-Hartree–Fock results in Table 2), and is further reduced by 0.7 kcal/mol upon zero-point correction. In C_3 -symmetric **1b**, the hydronium protons are located nearly equidistant to the crown O atoms (shortest O \cdots H separations of 2.008 and 2.036 Å), and the pyramidal structure of the hydronium ion is retained.

During the MD simulations (see below), frequent inversion of the hydronium ion was observed. The corresponding structure with a planar H_3O^+ was located as a transition state on the PES

Scheme 1



(**1c** in Chart 3). In near- C_{3v} symmetric **1c** the planar H_3O^+ moiety (angle sum at O 360°) is located halfway between the upper and lower O_3 planes of the crown ether and forms three linear hydrogen bonds ($O-H\cdots O$ angle 175°) with short $H\cdots O$ contacts (1.727 \AA). The inversion process starting from **1a** via **1c** leads to a structure where, in the orientations shown in Charts 2 and 3, the O(hydronium) atom lies below the plane of the lower three O(crown) atoms, which remain the hydrogen-bond acceptors. The resulting structure (Scheme 1) is equivalent to **1a'**, to which it is related by a rotation about a pseudo- C_2 axis of the crown ether substructure.

The computed inversion barrier via **1c** is very low on the PES, ca. 1.0–1.4 kcal/mol (BLYP and MP2 values, respectively; see Table 2), and is further reduced by zero-point effects to ca. 0.2–0.6 kcal/mol. Hydronium inversion in **1** is thus indicated to be an extremely facile process, faster even than in free H_3O^+ , for which barriers on the PES of 1.7 and 2.3 kcal/mol are obtained with BLYP and MP2, respectively, and should indeed be a much faster process than rotation via **1b**.

Given the ease of H_3O^+ planarization in **1a**, it appeared conceivable that bifurcated hydrogen bonds might actually be more favorable with a planar hydronium moiety. Therefore, a corresponding stationary point was located by imposing D_3 symmetry (**1d** in Chart 3). With its two imaginary frequencies, **1d** was characterized as a second-order saddle point for simultaneous inversion and rotation of the H_3O^+ moiety. This point is 6.3 kcal/mol higher in energy than **1a**, or 1.7 kcal/mol above **1b**, and should thus be less relevant for the dynamics within the complex.

Of the computed vibrational frequencies of **1a**–**1d**, those with the highest IR intensities are included in Table 1. Modes associated with the crown ether moiety have quite similar frequencies for all species studied. Vibrations centered on H_3O^+ are in the general range observed for other hydronium salts.²⁶ The most intense IR band, the asymmetric OH stretch, could be of some diagnostic value, as quite different ranges are computed for bifurcated (**1b**, **1d**) and linear (**1a**, **1a'**, **1c**) hydrogen bonds, around 3100–3200 and 2900 cm^{-1} , respectively. The latter value compares more favorably to the data reported for $(Zn/Mn)O_4^-$ salt of **1**, $\approx 2950 \text{ cm}^{-1}$.^{22,27} More theoretical and experimental work, however, is required for definite assignments.

Molecular Dynamics Simulations. During a 5 ps CPMD simulation of **1** at ca. 300 K, the hydronium ion remains hydrogen-bonded to the same set of O(crown) atoms. During that time, four H_3O^+ inversion processes are observed, which, as far as the H_3O^+ binding mode is concerned, interconvert

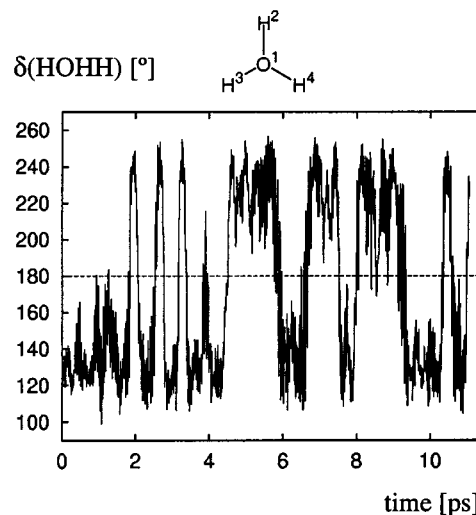


Figure 1. Evolution of the $H^2O^1H^3H^4$ dihedral angle with the simulation time; each crossing of 180° constitutes an inversion process of the hydronium ion.

structures corresponding to **1a** and **1a'**. When the simulation was repeated at a higher temperature, on average around 340 K, the frequency of inversion roughly doubled (nine events during the first 5 ps). In Figure 1, this process is monitored by the HOHH dihedral angle as a function of time.

In addition to these inversions, one rotation via a bifurcated structure resembling **1b** occurred after about 4 ps, and a second one, in the same direction, after another 6 ps. Clearly, only limited conclusions can be drawn from these rare events, which, however, confirm that H_3O^+ inversion is much more facile than rotation. Interestingly, in the course of the first rotation, the proton switch from one O_3 set to the other did not proceed fully synchronously as would be expected from the C_3 symmetric transition state. Rather, two of the hydronium protons jumped essentially simultaneously and the third one lagged behind, not hopping for another 0.3 ps. This is illustrated in Figure 2, a plot of the three sets of breaking and forming $O\cdots H$ bond distances. On the other hand, the second rotation (not shown) proceeded almost synchronously and was completed in less than 0.1 ps.

At this elevated temperature, the crown ether is very flexible. For instance, large fluctuations occur in the OCCO dihedral angles, the absolute values of which can vary between 33° and 100° around an average of 65° . However, no clear-cut correlation between crown ether dynamics and hydronium mobility is apparent.

The flexibility of **1** is also reflected in the broad distribution of $O(\text{hydronium})\cdots O(\text{crown})$ distances during the simulation, as illustrated by the corresponding pair correlation function $g_{OO}(r)$ ²⁸ (Figure 3). Note that significant contributions arise from distances larger than 3.2 \AA , i.e., about 0.4 \AA longer than in most solid-state structures where the conformational freedom is reduced.

In Figure 4, the average of the three $O(\text{hydronium})\cdots O'$ distances is monitored for 10 ps spanning both H_3O^+ rotation events, during which they change from hydrogen-bonded to nonbonded distances, and back. The concomitant elongation and

(26) (a) Gillard, R. D.; Wilkinson, G. *J. Chem. Soc.* **1964**, 1640. (b) Savoie, R.; Giguère, P. A. *J. Chem. Phys.* **1967**, *41*, 2698.

(27) Density-functional derived harmonic frequencies are often quite close to observed fundamentals due to favorable error compensation; see, for instance, ref 8.

(28) For the definition of the pair correlation function see, for example, Allen, M. P.; Tildesley, D. J. *Computer Simulation of Liquids*; Clarendon Press: Oxford, U.K., 1987.

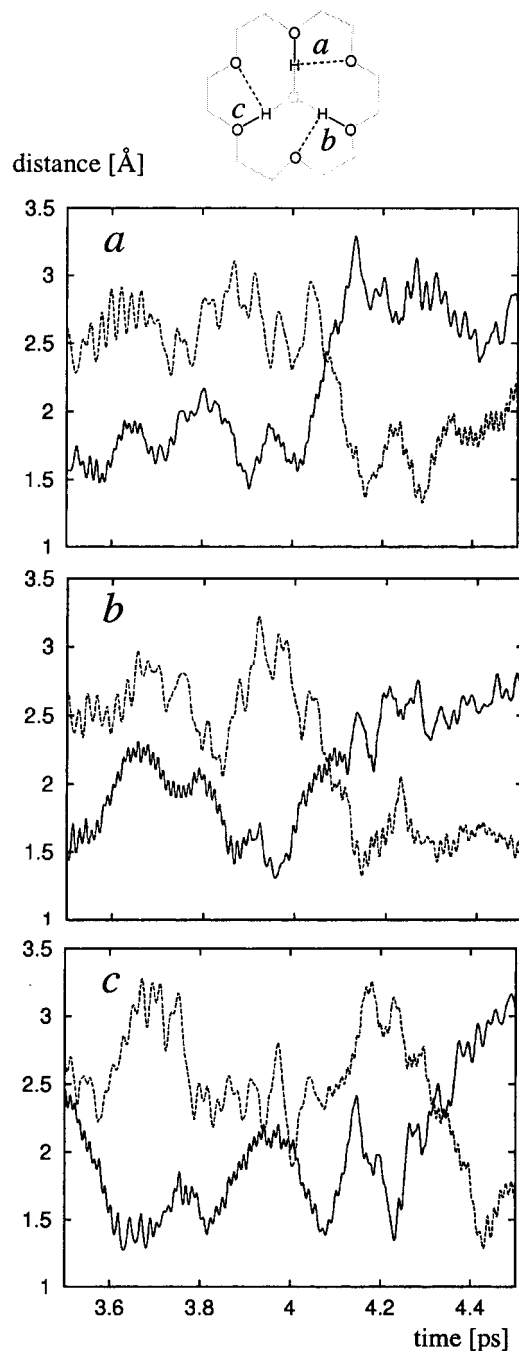


Figure 2. Monitoring of O...H bond distances involved in the first 120° rotation of the H₃O⁺ moiety, as observed in the MD simulation.

shortening, respectively, is clearly visible, as are the large fluctuations over time that give rise to the broad pair-correlation function in Figure 3. Also included in Figure 4 is the standard deviation of the three O(hydronium)···O' distances from their average value at each point. These data illustrate that the hydronium ion is not symmetrically coordinated during most of the time (though it is when averaged over the whole simulation) and that noticeable displacements away from the pseudo-C₃ axis can occur.

Discussion

Where Are the Hydronium Protons? The computational results provide a consistent answer to the title question concern-

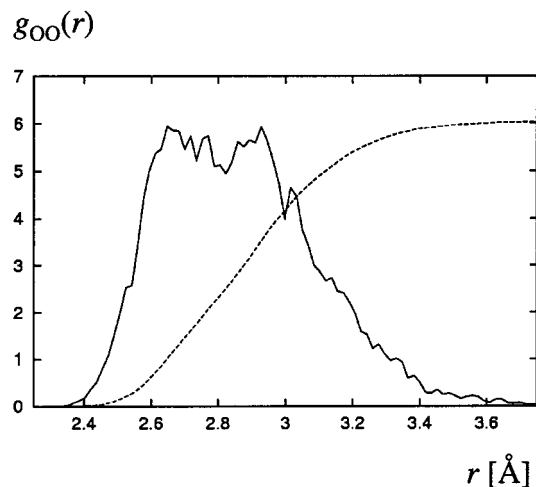


Figure 3. (—) Simulated O(hydronium)···O(crown) pair correlation functions $g_{OO}(r)$. (---) $n_O(r) = \rho \int g(r) 4\pi r^2 dr$, which integrates to the total number of oxygen atoms in a sphere with radius r around the O(hydronium) atom.

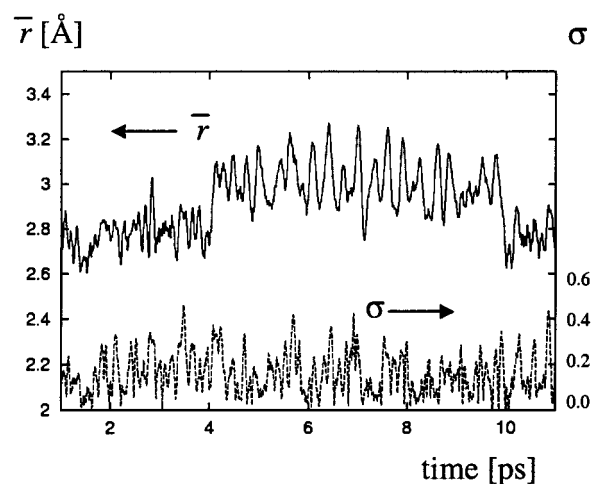


Figure 4. Evolution of the average of the three O(hydronium)···O' distances and the corresponding standard deviation with the simulation time.

ing the location of the protons in **1**: they are involved in essentially linear two-center hydrogen bonds as in **1a**. A bifurcated arrangement as in **1b** is higher in energy by ca. 4 kcal/mol (including ZPE) and is a transition structure for rotation of the H₃O⁺ moiety about its 3-fold axis. This energy difference is small when compared to the total binding enthalpy, −88.5 kcal/mol. The latter experimental number is difficult to reproduce computationally, as the absolute values based on post-Hartree–Fock results are larger by 5 (BLYP) to 10 kcal/mol (MP2 level, Table 2). A similar overestimation of MP2-derived binding energies has been noted for alkali cation/crown ether complexes.⁴ In contrast to the absolute complexation energies, the computations should describe relative energies between similar isomers or rotamers more accurately. Unlike the binding enthalpy, the energy difference between **1a** and **1b** is remarkably independent of the theoretical method (Table 2), and the value of ca. 4 kcal/mol should be reliable.

A similar value for this energy difference, 2.9 kcal/mol, is obtained for the related NH₄⁺/18c6 complex (**2**), where we could locate the corresponding stationary points **2a**, **2a'**, and **2b**.^{29,30} The experimental binding energy of NH₄⁺ is much smaller than that of H₃O⁺, by ca. 25 kcal/mol,³¹ and linear two-center hydrogen bonds have been observed in the solid state.³² The

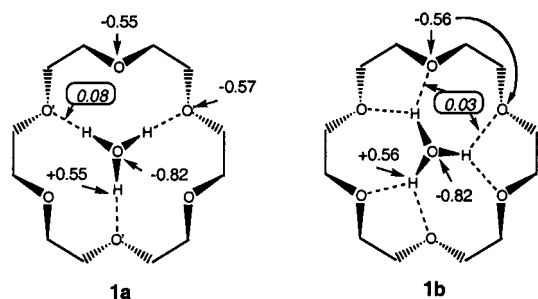


Figure 5. NPA charges and Wiberg bond indices (in boxes) of **1a** and **1b**, BLYP/II' level.

structures of NH_4^+ complexes in the crystal result from the interplay between intrinsic host–guest interactions and interactions between complexed NH_4^+ and the counterions such as halides or nitrate. Our computations suggest that the propensity for linear rather than bifurcated hydrogen bonds is an intrinsic property in both H_3O^+ and NH_4^+ complexes.

How tightly is the hydronium ion anchored to the crown ether during the dynamics? In typical hydrogen-bonded systems containing $\text{O}\cdots\text{H}\cdots\text{O}$ moieties, the $\text{O}\cdots\text{O}$ distance is smaller than 3.5 Å and the OH bond is directed toward the second oxygen atom such that the $\text{O}\cdots\text{H}\cdots\text{O}$ angle is larger than 140° .³³ During the simulations it occurred only very rarely that hydrogen bonds, according to these purely geometrical criteria, were ruptured, even at 340 K, and the average number of hydrogen bonds over 10 ps is well above 2.9. Despite the large flexibility of **1** illustrated by Figures 3 and 4, well-directed hydrogen bonds prevail for most of the time, consistent with the strong binding energy.

Why Are the Hydrogen Bonds Linear? On purely electrostatic grounds, the hydronium protons should be equidistant between two neighboring O(crown) atoms, as in **1b**, rather than placed unsymmetrically, as in **1a** (see $\text{H}\cdots\text{O}$ distances in Table 1). Natural population analysis (NPA)³⁴ indicates noticeable charge transfer from 18c6 to the H_3O^+ moiety in **1a**, 0.17e, but very similar charge densities at both coordinated and uncoordinated O(crown) atoms (Figure 5). The charge distribution is hardly altered upon H_3O^+ rotation from **1a** to **1b**.³⁵

A first indication of the reason for the observed directionality is provided by the calculated $\text{O}\cdots\text{H}$ bond orders with Wiberg's definition³⁶ (WBIs), a rough indicator for covalent interactions. A noticeable WBI of 0.08 per proton is found in **1a**, which is reduced to 0.03 (twice) in **1b** (Figure 5). Evidence for similar “incipient covalency” in related $\delta^-\text{O}\cdots\text{H}\cdots\text{O}^{\delta-}$ hydrogen bonds

involving anions has been obtained from topological analysis of experimental electron densities.³⁷

Closer inspection of the localized natural bond orbitals (NBOs)³⁴ reveals donor–acceptor interactions between the lone pairs on the O(crown) atoms and antibonding σ^*_{OH} orbitals of H_3O^+ .³⁸ When the corresponding elements of the Fock matrix in the NBO basis are deleted and one SCF cycle is performed,³⁴ the resulting energy of **1b** is indeed lower than that of **1a**. Quantitatively, this crude method affords a very large energy difference between the two structures, ca. 25 kcal/mol, but qualitatively, this result suggests that indeed specific orbital interactions are more stabilizing in **1a** than in **1b**. Similar donor–acceptor orbital interactions have been proposed to account for part of the binding energy of DNA base pairs (involving N and O lone pairs and σ^*_{NH} orbitals).^{39,40} In the latter systems, as in most complexes between highly polar hydrogen-bond donors and acceptors, these orbital effects are superseded by electrostatic interactions between the dipole (and higher) moments of the individual components. Such interactions being largely similar for **1a** and **1b**, it is indeed likely that orbital effects are the driving force for the stability of the former over the latter.

As a consequence, conventional force fields, which mainly rely on electrostatics to describe hydrogen bonds,⁴¹ should not be able to reproduce the energetic balance between **1a** and **1b** correctly. In fact, a typical force field such as Amber erroneously gives **1b** as minimum,⁴² also with atomic polarization.⁴³ For complexes with ammonium cations, MM calculations also give bifurcated minima,⁴⁴ but charge and polarization parameters can be chosen such that linear arrangements are preferred.⁴⁵

18c6 Catalyzes the Inversion of Its H_3O^+ Guest. In addition to rotation via the bifurcated transition state **1b**, inversion of the coordinated hydronium ion turned out to be another dynamical process, which to our knowledge has not been described for **1** before. This process came to our attention during the MD simulations, where it happened much more frequently than rotation. The inversion barrier of free H_3O^+ is low, 2.3

- (29) Relative energies at BLYP/II'/BLYP/6-31G*: 0.0, 0.7, and 2.9 kcal/mol for **2a**, **2a'**, and **2b**, respectively (0.0, 0.5, and 2.1 kcal/mol, respectively, including ZPE). Rotation of the guest should thus be faster in **2** than in **1**; it is possible that in the solid state the apparent interaction of NH_4^+ with the counterions locks **2** in the observed conformation, which corresponds to that in **2a'**.
- (30) A small barrier for NH_4^+ rotation in **2** has also been inferred from local density-functional computations: Ha, Y. L.; Chakraborty, A. K. *J. Phys. Chem.* **1992**, *96*, 6410–6417.
- (31) Meot-Ner (Mautner) M.; Sieck, L. W.; Liebman, J. F.; Scheiner, S. *J. Phys. Chem.* **1996**, *100*, 6445–6450.
- (32) For instance: (a) Pears, D. A.; Stoddart, J. F.; Fakley, M. E.; Allwood, B. L.; Williams, D. J. *Acta Crystallogr., Sect. C* **1988**, *44*, 1426. (b) Doxsee, K. M.; Francis, P. E., Jr.; Weakly, T. J. *Tetrahedron* **2000**, *56*, 6683–6691.
- (33) For instance: Schwegler, E.; Galli, G.; Gygi, F. *Phys. Rev. Lett.* **2000**, *84*, 2429–2432.
- (34) Reed, A. E.; Curtiss, L. A.; Weinhold, F. *Chem. Rev.* **1988**, *88*, 899–926.
- (35) Somewhat different atomic charges are obtained from Mulliken population analysis of **1a**, -0.42 and -0.45 for O(crown), -0.35 for O(hydronium), and $+0.34$ for H(hydronium).
- (36) Wiberg, K. *Tetrahedron* **1968**, *24*, 1083–1096.

- (37) In solid KHC_2O_4 : Macchi, P.; Iversen, B. B.; Sironi, A.; Chakoumakos, B. C.; Larsen, F. K. *Angew. Chem., Int. Ed.* **2000**, *39*, 2719–2722; see also references therein.
- (38) The existence of such orbital interactions was first suggested on the basis of CNDO/2 results: Yamabe, T.; Hori, K.; Fukui, K. *Tetrahedron* **1997**, *53*, 1065–1072.
- (39) Guerra, C. F.; Bickelhaupt, F. M.; Snijders, J. G.; Baerends, E. J. *Chem. Eur. J.* **1999**, *5*, 3581–3594.
- (40) For a recent account on ab initio studies of hydrogen bonds in general, see Del Bene, J. E.; Jordan, M. J. T. *J. Mol. Struct. (THEOCHEM)* **2001**, *573*, 11–23 and references therein.
- (41) (a) Lii, J.-H.; Allinger, N. L. *J. Comput. Chem.* **1998**, *19*, 1001–1016. (b) Hay, B. P.; Hancock, R. D. *Coord. Chem. Rev.* **2001**, *212*, 61–67. (c) Ferguson, D. M.; Kollman, P. A. *J. Comput. Chem.* **1991**, *12*, 620–626. (d) Ewig, C. S.; Thacher, T. S.; Hagler, A. T. *J. Phys. Chem. B* **1999**, *103*, 6998–7014.
- (42) Optimizations were performed with AMBER 5.0 (Case, D. A.; Pearlman, D. A.; Caldwell, J. C.; Cheatham, T. E., III; Ross, W. S.; Simmerling, C. L.; Darden, T. A.; Merz, K. M.; Stanton, R. V.; Cheng, A. L.; Vincent, J. J.; Crowley, M.; Ferguson, D. M.; Radmer, R. J.; Seibel, G. L.; Singh, U. C.; Weiner, P. K.; Kollman, P. A. *AMBER5*, University of California, San Francisco, 1997) with the parameters from the AMBER force field (Cornell, W. D.; Cieplak, P.; Bayly, C. I.; Gould, I. R.; Merz, K. M.; Ferguson, D. M.; Spellmeyer, D. C.; Fox, T.; Caldwell, J. W.; Kollman, P. A. *J. Am. Chem. Soc.* **1995**, *117*, 5179–5197), with different combinations of atomic charges on H_3O^+ [O(0.0)–H(+0.333); O(–0.764)–H(+0.588)] and ESP charges on the crown [O(–0.404), C(0.244), H(–0.021)]: Auffinger, P.; Wipff, G. *J. Am. Chem. Soc.* **1991**, *113*, 5976–5988.
- (43) Atomic polarizabilities (α_{O} and α_{H} = 0.526 and 0.170 Å³, respectively) were taken from Chang, T. M.; Dang, L. X. *J. Chem. Phys.* **1996**, *104*, 6772–6783.
- (44) Rüdiger, V.; Schneider, H.-J.; Solov'ev, V. P.; Kazachenko, V. P.; Raevsky, O. A. *Eur. J. Org. Chem.* **1999**, 1847–1856.
- (45) Gehin, D.; Kollman, P. A.; Wipff, G. *J. Am. Chem. Soc.* **1989**, *111*, 3011–3023.

kcal/mol based on the MP2⁴⁶ energies. Intuitively one would expect a floppy molecule to become more rigid upon complexation to a crown ether. According to our computations, however, the opposite is the case for **1**: H₃O⁺ inversion is indicated to be facilitated in the complex with 18c6, and the MP2-derived barrier via **1c** is reduced to 1.4 kcal/mol. The stronger binding by 18c6 of planar vs pyramidal H₃O⁺ is also reflected in the shorter H···O(crown) distances in **1c** vs **1a**, 1.727 vs 1.762 Å (Table 1).

Given the very low inversion barrier, it might even be possible that the lowest vibrational mode along the inversion coordinate in **1a** is already at or slightly above this barrier on the PES.⁴⁷ In such a case, one could expect a broad probability distribution of the O(hydronium) atom along the 3-fold axis, with significant if not major contributions from positions near the center. In this context it is interesting to note that, in some of the X-ray crystallographic studies, this atom was found to have large thermal amplitudes⁴⁸ or to be disordered over equivalent positions at opposite sides of the crown ether.²³ Clearly, more sophisticated calculations incorporating nuclear quantum effects⁴⁹ would be needed to address this issue. It is also quite likely that the mean position of the O(hydronium) atom could be sensitive to the surrounding medium (see below).

The receptor 18c6 is quite remarkable in its affinity toward H₃O⁺, as it provides strong binding for this substrate, combined with energetic lowering of a salient transition state. These are features normally associated with catalysts. Thus, 18c6 can be viewed as a catalyst for H₃O⁺ inversion.

Interaction with the Surrounding Medium. In solid-state structures not involving crown ethers, such as acid hydrates, the H₃O⁺ protons are usually anchored to three anions, locking, by extended hydrogen-bond networks, the hydronium ion in a tetrahedral environment that hinders inversion.⁵⁰ For the cationic complex **1** in condensed phase, interaction with its counteranions should be weak, since the electrophilic protons are tucked away in the crown “pocket”, which effectively shields them. In addition, anions are repelled by the electron-rich O(hydronium) atom. Due to its overall positive charge, complexed H₃O⁺ is also not a good hydrogen-bond acceptor. It should thus be quite hydrophobic, more so than, for instance, the corresponding alkali metal or NH₄⁺ complexes, where the cation is more exposed and can coordinate polar ligands, solvent molecules, or counterions. Structure and dynamics of **1** in solution should thus be similar to that described by our gas-phase computations.

However, given the flat PES for isolated **1**, even weak interactions with remote dipoles or ions could be important. For instance, when a Cl[−] counterion is placed above the crown in **1a**, approaching from the same side as the complexed hydronium ion, the latter inverts in the course of a BLYP/6-31G* optimization, and Cl[−] remains attached to the crown ether via

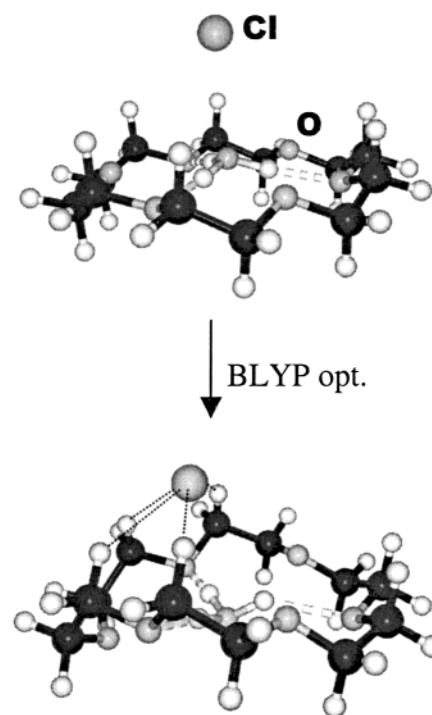


Figure 6. Input and final, optimized structure of a **1**·Cl[−] complex.

several Cl[−]···H—C interactions, causing significant conformational distortions (Figure 6). In solid-state structures of H₃O⁺/18c6 complexes, associated counterions are generally large and soft and are located beyond contact distances with the hydronium ion.² Further theoretical work would be desirable to elucidate the detailed effect of counterions and the medium on structure and dynamics of **1**.⁵¹ Special attention should be called to circumstances that require a description of the nuclear dynamics beyond the classical treatment employed so far.⁴⁹

Conclusions

We have presented a quantum-mechanical study of the static and dynamic features of H₃O⁺ binding with 18-crown-6. Two arrangements with three linear (two-center) O—H···O(crown) hydrogen bonds are found to be of similar stability, while a 60° rotation of H₃O⁺ to form “delocalized” bifurcated (three-center) hydrogen bonds leads to a transition state with higher energy (>4 kcal/mol). The inversion of pyramidal H₃O⁺ within the complex is found to be a more facile process (<2 kcal/mol), constituting a “catalyzed” fluxional process not recognized so far. These features explain the dynamic behavior of the complex in the gas phase, obtained from an 11 ps CPMD simulation at ca. 340 K. The hydronium cation undergoes several (about 16) inversions, switching between the “equatorial” lone pairs of the two sets of nonequivalent ether oxygens, but completes only two rotations of about 120°. These static and dynamic results contrast with those obtained by classical force field approaches using 1–6–12 pairwise additive potentials,

(46) Practically the same number is obtained at the MP2 level with a larger basis set: Rodwell, W. R.; Radom, L. *J. Am. Chem. Soc.* **1981**, *103*, 2865–2866.

(47) Among the BLYP/6-31G* harmonic vibrational frequencies of **1a**, the corresponding “umbrella” $\delta_{oop}(\text{H}_2\text{O})$ mode appears at 1051 cm^{−1} (Table 1), which would correspond to ca. 1.5 kcal/mol in ZPE.

(48) For instance: Shoemaker, C. B.; McAfee, L. V.; Shoemaker, D. P.; DeKock, C. W. *Acta Crystallogr., Sect. C* **1986**, *42*, 1310–1313.

(49) For instance, via path-integral methods; for a recent application see Marx, D.; Tuckerman, M. E.; Hutter, J.; Parrinello, M. *Nature* **1999**, *397*, 601–604.

(50) See, for instance, Lundgren, J.-O.; Olovsson, I. In *The Hydrogen Bond. II. Structure and Spectroscopy*; Schuster, P., Zundel, G., Sandorfy, C., Eds.; North-Holland: Amsterdam, 1996; pp 472–526.

(51) A reviewer pointed out that H₃O⁺ could be planar and with bifurcating H bonds if sandwiched between two 18c6 moieties. There is evidence from conductance and NMR studies for the occurrence of such a 1:2 complex (Amini, M. K.; Shamsipur, M. *J. Solution Chem.* **1992**, *21*, 275–288). At the BLYP/6-31G* level, such a H₃O(18c6)₂⁺ complex could be located in D₃ symmetry (that is, with a planar H₃O⁺ placed symmetrically between two crown ether molecules) but is 13.8 kcal/mol above **1a** + 18c6. The actual 1:2 complexes may involve, for instance, H₅O₂⁺ as bridging ligand between the crown ethers.

with or without allowing for polarization, which favor bifurcated hydrogen bonds. The observed directionality of these bonds can be rationalized by orbital interactions between lone pairs on the O(crown) atoms and hydronium σ^*_{OH} antibonding orbitals. Possible medium effects notwithstanding, these findings are important for understanding the role of topologically constrained environment of H_3O^+ and related ether lone-pair orientations on the static *and* dynamic aspects of strong hydrogen-bonding interactions.

Acknowledgment. M.B. thanks Professor W. Thiel for his continuing support, the Deutsche Forschungsgemeinschaft for

a Heisenberg fellowship, and Professor Dr. G. Wipff for an invitation to spend a one-month sabbatical in Strasbourg. G.W. thanks A. Varnek for useful discussions. Computations were performed on Compaq XP1000 and ES40 workstations at the MPI Mülheim.

Supporting Information Available: Geometries and BLYP/6-31G* energies in the form of Gaussian archive entries. This material is available free of charge via the Internet at <http://www.pubs.acs.org>.

JA012428J